Polarization-dependent thin-film wire-grid reflectarray for terahertz waves

Tiaoming Niu,[1,2] Aditi Upadhyay,[3] Withawat Withayachumnankul,[1,4] Daniel Headland,[1] Derek Abbott,[1] Madhu Bhaskaran,[3] Sharath Sriram,[3] and Christophe Fumeaux[1,a)]
[1]*School of Electrical and Electronic Engineering, The University of Adelaide, Adelaide, South Australia 5005, Australia*
[2]*School of Information Science and Engineering, Lanzhou University, Lanzhou 730000, People's Republic of China*
[3]*Functional Materials and Microsystems Research Group, RMIT University, Melbourne, Victoria 3001, Australia*
[4]*Interdisciplinary Graduate School of Science and Engineering, Tokyo Institute of Technology, 2-12-1-S9-3, Ookayama, Meguro-ku, Tokyo 152-8552, Japan*

(Received 2 April 2015; accepted 14 July 2015; published online 23 July 2015)

A thin-film polarization-dependent reflectarray based on patterned metallic wire grids is realized at 1 THz. Unlike conventional reflectarrays with resonant elements and a solid metal ground, parallel narrow metal strips with uniform spacing are employed in this design to construct both the radiation elements and the ground plane. For each radiation element, a certain number of thin strips with an identical length are grouped to effectively form a patch resonator with equivalent performance. The ground plane is made of continuous metallic strips, similar to conventional wire-grid polarizers. The structure can deflect incident waves with the polarization parallel to the strips into a designed direction and transmit the orthogonal polarization component. Measured radiation patterns show reasonable deflection efficiency and high polarization discrimination. Utilizing this flexible device approach, similar reflectarray designs can be realized for conformal mounting onto surfaces of cylindrical or spherical devices for terahertz imaging and communications. © *2015 AIP Publishing LLC*. [http://dx.doi.org/10.1063/1.4927386]

Owing to the advantages of a flat profile and high efficiency, reflectarrays have been widely implemented across the electromagnetic spectrum,[1] from microwave,[2,3] millimeter-wave,[4,5] terahertz[6,7] to optics.[10–13] A typical reflectarray is composed of three layers: a top layer with resonant elements arranged periodically with a beam-forming phase distribution, a dielectric spacer, and a metal ground plane. As one of the possible functions of a reflectarray, waves incident on its surface can be deflected into an off-specular direction. Because of the presence of a full metal ground plane, the incident electric field can only be re-radiated backwards into free space after interacting with the reflectarray. In this letter, a terahertz reflectarray using patterned double-layer metallic wire-grid geometry is proposed to realize two polarization-dependent functions: (i) reflective deflection for the incident polarization parallel to the grid and (ii) normal transmission for the orthogonal polarization—therefore, it can be considered as a combination of a reflectarray and a wire-grid polarizer.[8] This reflectarray structure is fabricated on a free-standing flexible polymer substrate. Hence, the structure is flexible and stretchable.

A schematic diagram of the unit cell and the layout for the proposed reflectarray is given in Fig. 1. The array is composed of periodically arranged identical subarrays. Each subarray contains a certain number of subwavelength unit cells, and each cell is made of a resonant element on the ground plane with a flexible polymer polydimethylsiloxane (PDMS)[14] as a dielectric spacer. This individual resonant element is formed by grouping thin gold strips together in a square shape, while the ground plane is made of continuous gold strips.[9] All the gold strips for both the top and bottom layers have a width of 5 μm and are uniformly arranged with an inter-strip spacing of 5 μm. The size of the unit cell is fixed at $a = 140$ μm and the thickness of the PDMS dielectric layer is $h = 20$ μm. To improve the structural strength, a supporting layer of PDMS with a thickness of 100 μm is included under the ground plane. For clarity, this layer is not included in Fig. 1.

The proposed unit cell shown in Fig. 1(a) is simulated with the commercial software package, Ansys HFSS. A plane-wave excitation with a Floquet port and master-slave boundary conditions are applied for investigating the phase and magnitude responses of the unit cell in a uniform array. In the terahertz regime, the dissipation loss in gold caused by its finite conductivity and the dispersion require a realistic metal model to describe its performance. At 1 THz, the surface impedance of gold[15] obtained from a Drude model is $Z_{Au} = 0.287 + 0.335j$ Ω/sq. The relative permittivity and loss tangent of PDMS[14] adopted from independent measurement are $\epsilon_r = 2.35$ and $\tan\delta = 0.06$, respectively. For incident waves with a polarization parallel to the strips, denoted as the TE polarization, the structure performs as a reflectarray. Here, each group of thin strips on the top layer behaves as polarization-dependent equivalent of a patch resonator. When the length of the equivalent square patch is varied from 20 μm to 135 μm, the number of strips discretely increases from 2 to 14, as obtained by rounding the value of $l/10$ to the next integer. Over this length variation, a reflection phase range of over 300° is achieved for the TE polarization with acceptable efficiency, as shown in Fig. 2.

a)cfumeaux@eleceng.adelaide.edu.au

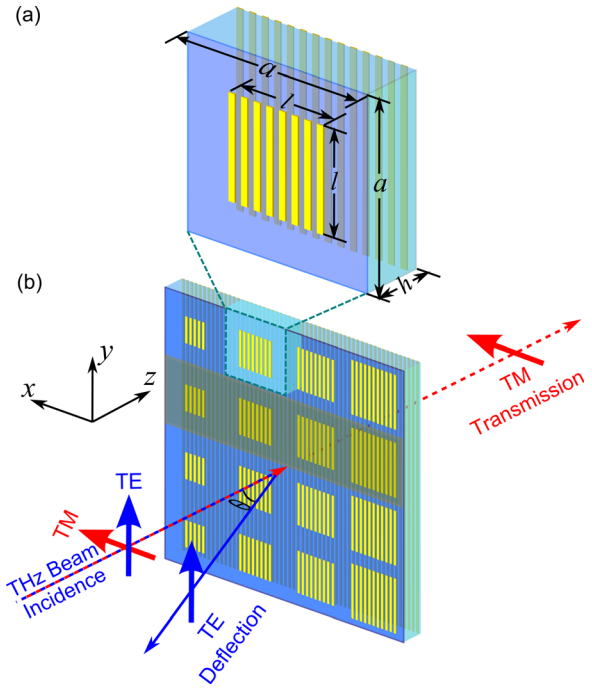

FIG. 1. A schematic diagram of the unit cell and the layout of the reflectarray. Each radiating element is composed of metal strips to form a polarization-dependent patch resonator, and the ground plane is made of a metallic wire grid. The strips for both the radiating element and the ground plane have the same width of 5 μm, and the gap between the adjacent strips is 5 μm. (a) The unit cell with a width of $a = 140\,\mu$m and a thickness of $h = 20\,\mu$m. (b) A part of the reflectarray showing 4 subarrays with each subarray being composed of 4 unit cells with different sizes of radiating elements. The shaded zone specifies one of the subarrays. The polarization-dependent functions are indicated with blue and red arrows.

The highest reflection loss of about −5 dB takes place at the resonant size of the wire-grid patch, for a length l of around 81 μm. For the excitation with the TM polarization (also shown in Fig. 2), regardless of the patch size, the transmission amplitude and phase remain nearly constant, with a small loss introduced by the dielectric PDMS substrate. Importantly, the device does not induce polarization conversion. The transmitted energy of less than −26 dB for the TE polarization and the reflected energy of around −11 dB for the TM polarization are insignificant and are not presented in Fig. 2.

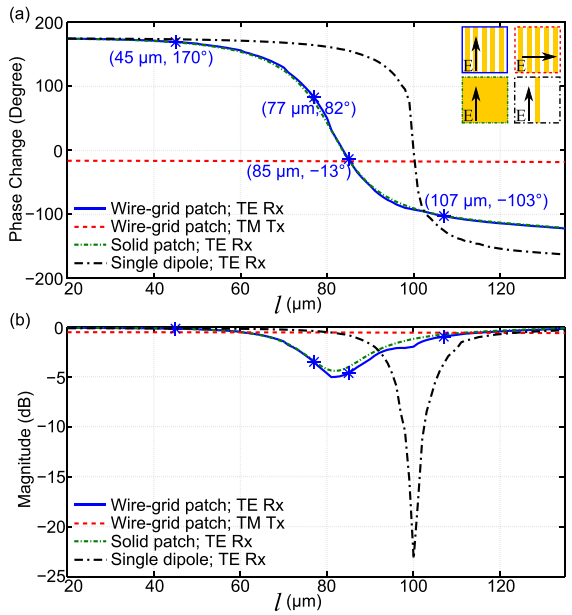

FIG. 2. Phase and magnitude responses of the unit cell for both the TE and TM polarized incident waves. (a) Phase response and (b) magnitude response. The four marks on the phase and magnitude curves indicate the selected radiating elements for defining a subarray that completes one full phase cycle.

For comparison, the reflection phase and magnitude responses of equivalent resonators realized with solid patches and single dipoles with a width of 5 μm, both on a grating ground plane, are also displayed in Fig. 2. The wire-grid patch offers similar phase and magnitude responses as those of the solid patch for the TE polarization. However, for the TM polarization, the solid patch has much lower transmission efficiency that reduces from −0.4 dB to −10 dB when the patch size increases from 20 μm to 135 μm (this result is not included in Fig. 2). On the other hand, the phase curve of the single dipole resonator has a remarkably steep slope and significantly higher loss due to a high-Q resonance. Therefore, using the wire-grid patch resonator as radiating elements combines the advantages of high efficiency of the patch (for the TE polarization) with the polarization dependence of the dipole.

As a proof of concept, a polarization-dependent reflectarray is designed to deflect a normally incident TE polarization into a predefined direction while transmitting the TM polarization. For simplicity, the array is constructed as periodic arrangement in subarrays, designed based on the phase response of the unit cell as shown in Fig. 2. The deflection angle θ is determined by the progressive phase change of adjacent wire-grid patches according to the formula[16]

$$\theta = \arcsin\left(\frac{\lambda_0}{d}\right) = \arcsin\left(\frac{\Delta\phi\lambda_0}{2\pi a}\right), \tag{1}$$

where λ_0 is the operation wavelength and $d = 2\pi a/\Delta\phi$ is the size of the subarray, while $\Delta\phi$ is the progressive phase change between adjacent cells and a is the size of the unit cell. The value of $\Delta\phi$ can be chosen arbitrarily. In this letter, we choose $\Delta\phi = \pi/2$ so that a complete phase cycle of 2π is achieved with subarrays of 4 elements. Therefore, the length of the subarray is given by $d = 4a = 560\,\mu$m to achieve a deflection angle of $\theta = 32.4°$ at 1 THz. The size and corresponding phase and amplitude responses of the 4 elements are marked in Fig. 2(a). It is noted that the fabrication tolerance demands the lengths of the strips for the radiating elements to be rounded to discrete values in microns, and thus, small phase inaccuracies can be expected particularly where the phase response is highly sensitive to a change in the wire-grid patch length, i.e., in the section of the phase curve with a steep slope.

The simulated scattered field distributions for the TE and TM polarized plane wave excitations are demonstrated in Figs. 3(a) and 3(b), respectively. When the normally incident plane wave is polarized in the direction parallel to the strips (TE), the designed structure functions as a reflectarray deflecting the incident waves into the predesigned direction $\theta = 32.4°$ off the direction of specular reflection. From Fig. 3(a), the energy leaked to the other side of the structure is relatively small. For the plane wave with polarization

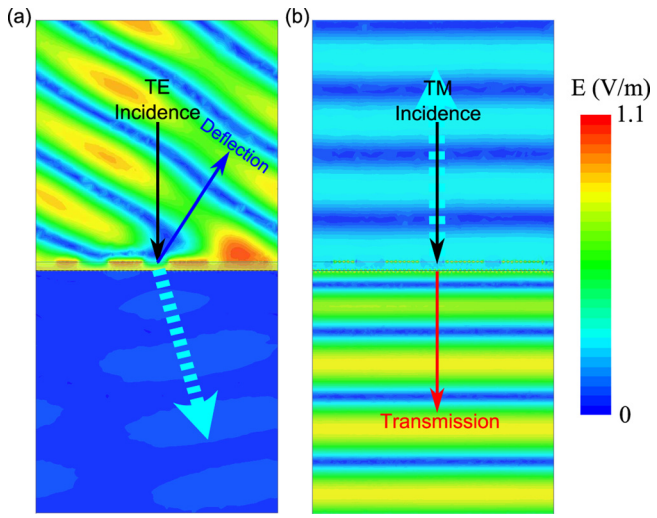

FIG. 3. Instantaneous scattered fields from the reflectarray in the (a) TE and the (b) TM polarizations at 1 THz.

perpendicular to the strips (TM), the structure allows transmission with minimal attenuation caused by the dielectric dissipation and reflection losses.

The designed reflectarray has been fabricated for validation of the proposed functionality. The optical micrographs of a small area in Fig. 4 show the details of the gold wire-grid patches and the wire-grid ground plane. The entire sample has a size of 50.4 mm × 50.4 mm and contains 90 × 360 periodically arranged subarrays. The sample is measured with a terahertz time-domain spectroscopy (THz-TDS) system, Tera K15 developed by Menlo Systems GmbH. Three measurement configurations are necessary to characterize the angular response of the sample (see the supplementary material for the measurement setup).[17] The first two configurations are set to collect the radiation patterns around the sample for normal incidence in the TE and TM polarizations. Because of the blind zone around the emitter, a third configuration is necessary to measure the specular reflection for the TE wave, which is achieved by rotating the sample with an angle of 20° while the emitter remains positioned at the same point as in the previous measurements. All the measurements are normalized using the air reference in transmission to remove system dependency.

For the normally incident beam, the measured normalized radiation patterns at the design frequency of 1 THz are

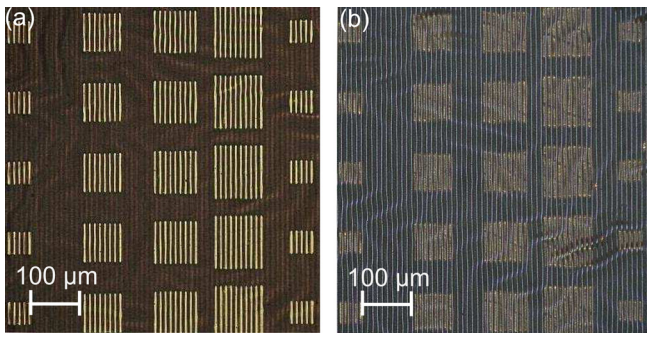

FIG. 4. Optical micrographs of a part of the fabricated sample. (a) The gold wire-grid patches of several subarrays located on the front side of the sample. (b) Back side showing the gold wire-grid ground plane (through a 100 μm thick layer of PDMS).

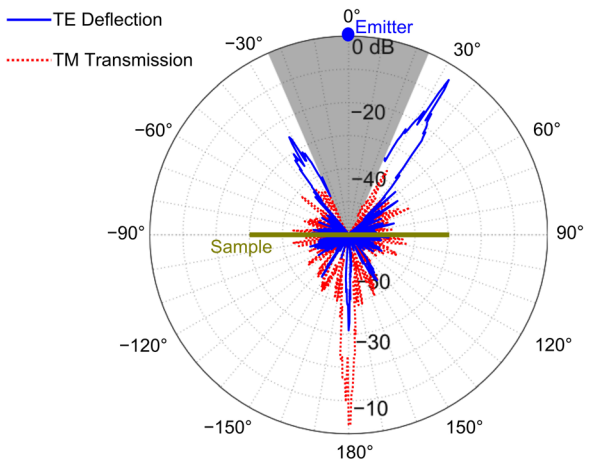

FIG. 5. Normalized radiation patterns at 1 THz for the TE (blue solid line) and TM (red dotted line) polarized waves on a logarithmic scale. The emitter antenna is located at 0°, and the collimated broadband terahertz beam normally impinges on the surface of the sample. The detector scans the angular range clockwise from 25° to −25° with an angular resolution of 0.5°. The minimum clearance between the emitter and the detector is 25°, and the angular clearance range is indicated by the grey zone.

presented in Fig. 5. When the polarization of the excitation is parallel to the wire-grid strips, the maximum deflection at the angle of 33° is observed with an efficiency of −4.1 dB and a polarization purity of at least −30 dB, as shown with the blue solid line. In contrast, the TM wave orthogonal to the strips is primarily transmitted through the sample with a normalized maximum amplitude of −2.2 dB as shown by the red dotted line in Fig. 5. In addition, the spectral characteristics of the reflectarray for normal incidence are demonstrated in Fig. 6, where the normalized magnitude is plotted in logarithmic scale as a function of frequency and scan angle. For the TE polarization as illustrated in Fig. 6(a), a strong deflection appears around the specified frequency in the designed

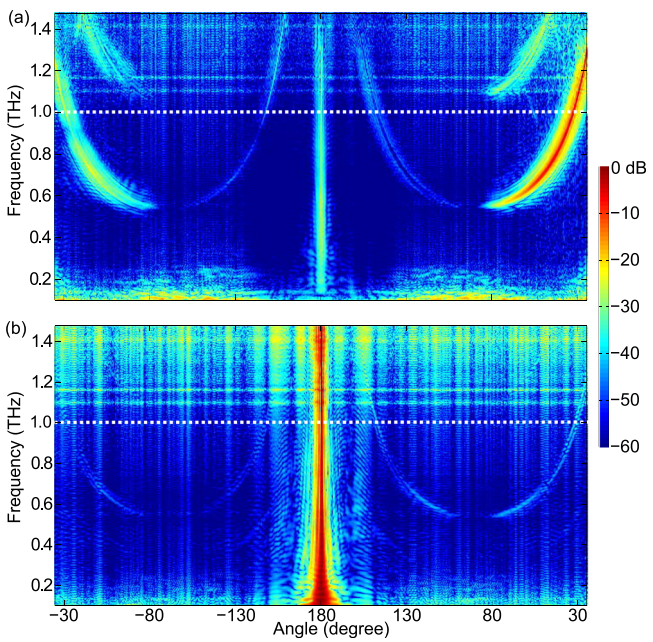

FIG. 6. Normalized scattered field as a function of the frequency and scan angle for the (a) TE and (b) TM polarizations. White dotted lines at 1 THz in (a) and (b) correspond to the radiation patterns for the TE and TM polarizations, respectively, shown in Fig. 5.

direction. Above and below the optimal frequency of 1 THz, the deflection efficiency degrades progressively. The deflection angle reduces with an increase in the operation frequency, i.e., as expected from the phenomenon of beam squint with frequency.[18] In addition to the main deflection lobe, minor lobes are observed in the forward and backward directions as a result of diffraction from the periodic configuration in subarrays. The corresponding results for the TM excitation are given in Fig. 6(b). For this polarization, the array is almost transparent to the incident waves in the measurable frequency range. The transmission magnitude is slightly reduced because of the reflection and dissipation losses. Small grating lobes with amplitude below −30 dB can be observed.

In the case of the TE obliquely incident excitation with an angle of 20°, the radiation pattern at the targeted frequency of 1 THz and the scattered field around the sample at different frequencies are demonstrated in Figs. 7(a) and 7(b), respectively. At 1 THz, the maximum deflection takes place at the off-normal angle of 61.5°, which is consistent with the theoretical expectation according to the formula[19]

$$\sin\theta_r = \sin\theta_i + \lambda_0/d, \tag{2}$$

where $\theta_i = 20°$ is the angle of incidence and θ_r corresponds to the deflection angle with respect to the normal. The calculated angle for the deflection is $\theta_r = 61.4°$. Therefore, the angle between the emitter and the detector for the maximum deflection should be $\theta_r + \theta_i = 81.4°$. In terms of power, the deflection magnitude is larger than the specular reflection magnitude by 12 dB. The spectral performance of the sample with the oblique TE polarized incident wave is shown in Fig. 7(b). In the frequency range lower than 0.8 THz, the sample can be regarded as a mirror and the incident beams are mostly reflected into the specular direction. At higher frequencies, the deflection becomes dominant and then reaches the maximum around the desired direction at 1 THz. At frequencies above 1 THz, the main deflection lobe attenuates gradually while the specular reflection becomes stronger.

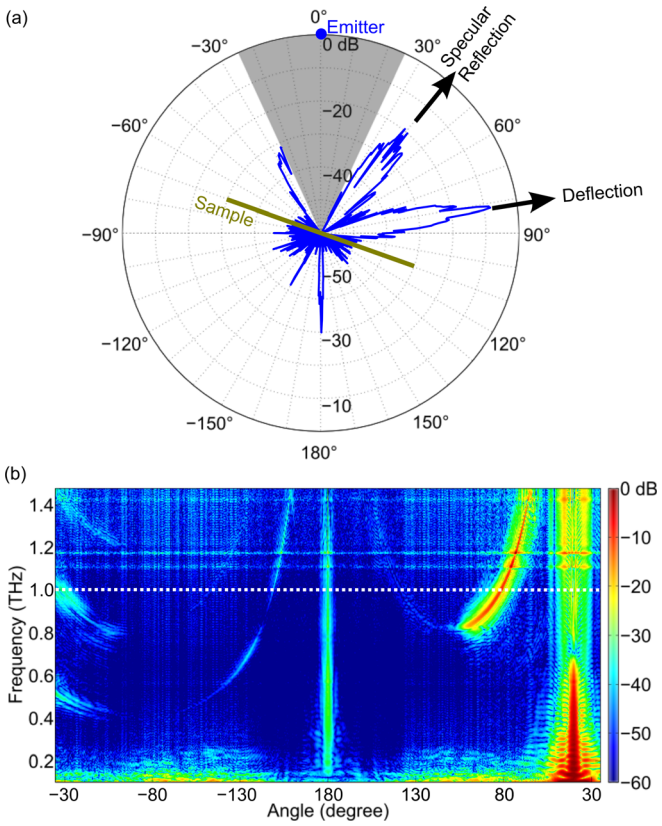

FIG. 7. Reflectarray response for the TE excitation with an oblique incident angle of 20° on a logarithmic scale. The emitter antenna is located at 0°, and the normal vector of the sample is toward 20°. (a) Radiation pattern at 1 THz. The grey zone indicates the angular clearance. (b) Normalized scattered field as a function of the frequency and scan angle. White dotted line at 1 THz corresponds to the radiation pattern in (a).

As the structure is stretchable, the function of beam steering can be achieved by mechanically stretching the reflectarray within a certain range. Preliminary measured results of the stretched sample indicate that the magnitude of the main lobe decreases and its direction moves away from the designed angle, while the magnitude of grating lobes increases. If a frequency-dependent linear phase response is achieved from broadband radiating resonators such as single-layered multi-resonant dipoles, beam steering with high performance can be achieved with the design concept demonstrated in this work. Owing to the flexible characteristics, the reflectarray can be conformally mounted onto a device with slightly curved surface to have a similar radiation pattern with a slight reduction in gain.[20] Because the pattern of each radiating element is normal to the local surface, the beamwidth of the conformal reflectarray is expected to be wider than its planar counterpart. For an improved design with no reduction of performance for curved surfaces, sophisticated phase synthesis approaches can be adopted.[21]

In conclusion, the concept of reflectarray based on the metallic wire-grid configuration has been numerically and experimentally validated in the terahertz regime. The combined polarization-dependent functions of reflective deflection and transmission are realized by the same structure. In the TE mode, a deflection efficiency of −4.1 dB is achieved. On the other hand, the TM waves can be transmitted through the reflectarray with a minimal change in amplitude. We note a small shift in the micro-fabricated wire-grid patches as a result of the mask preparation. Despite that imperfection, the sample still performs as expected, which further confirms the robustness of the design. Owing to the flexible characteristics, similar reflectarray configurations can be designed to be conformally mounted onto devices with an uneven surface.[22] In addition, the proposed concept of reflectarray can be extended to polarization-dependent reflective and transmissive deflection[23–26] by adding more layers of resonant elements onto the backside of the sample.

Tiaoming Niu acknowledges support from the Fundamental Research Funds for the Central Universities (Grant No. LZUJBKY-2014-43). Derek Abbott and Christophe Fumeaux acknowledge the ARC Future Fellowship funding scheme under FT120100351 and FT100100585, respectively.

[1]J. Huang and J. Encinar, *Reflectarray Antenna* (Wiley Online Library, 2008).
[2]E. Carrasco, M. Barba, J. A. Encinar, M. Arrebola, F. Rossi, and A. Freni, IEEE Trans. Antennas Propag. **61**, 3077 (2013).

[3]O. Bayraktar, O. A. Civi, and T. Akin, IEEE Trans. Antennas Propag. **60**, 854 (2012).
[4]P. Nayeri, M. Liang, R. S. García, M. Tuo, F. Yang, M. Gehm, H. Xin, and A. Elsherbeni, IEEE Trans. Antennas Propag. **62**, 2000 (2014).
[5]W. Hu, R. Cahill, J. Encinar, R. Dickie, H. Gamble, V. Fusco, and N. Grant, IEEE Trans. Antennas Propag. **56**, 3112 (2008).
[6]T. Niu, W. Withayachumnankul, A. Upadhyay, P. Gutruf, D. Abbott, M. Bhaskaran, S. Sriram, and C. Fumeaux, Opt. Express **22**, 16148 (2014).
[7]E. Carrasco, M. Tamagnone, and J. Perruisseau-Carrier, Appl. Phys. Lett. **102**, 104103 (2013).
[8]Z. Huang, E. P. Parrott, H. Park, H. P. Chan, and E. Pickwell-MacPherson, Opt. Lett. **39**, 793 (2014).
[9]N. K. Grady, J. E. Heyes, D. R. Chowdhury, Y. Zeng, M. T. Reiten, A. K. Azad, A. J. Taylor, D. A. Dalvit, and H.-T. Chen, Science **340**, 1304 (2013).
[10]A. Ahmadi, S. Ghadarghadr, and H. Mosallaei, Opt. Express **18**, 123 (2010).
[11]L. Zou, W. Withayachumnankul, C. M. Shah, A. Mitchell, M. Bhaskaran, S. Sriram, and C. Fumeaux, Opt. Express **21**, 1344 (2013).
[12]Y. Yifat, M. Eitan, Z. Iluz, Y. Hanein, A. Boag, and J. Scheuer, Nano Lett. **14**, 2485 (2014).
[13]E. Carrasco, M. Tamagnone, J. R. Mosig, T. Low, and J. Perruisseau-Carrier, Nanotechnology **26**, 134002 (2015).
[14]I. Khodasevych, C. Shah, S. Sriram, M. Bhaskaran, W. Withayachumnankul, B. Ung, H. Lin, W. Rowe, D. Abbott, and A. Mitchell, Appl. Phys. Lett. **100**, 061101 (2012).
[15]S. Lucyszyn, Piers Online **3**, 554 (2007).
[16]T. Niu, W. Withayachumnankul, B. S.-Y. Ung, H. Menekse, M. Bhaskaran, S. Sriram, and C. Fumeaux, Opt. Express **21**, 2875 (2013).
[17]See supplementary material at http://dx.doi.org/10.1063/1.4927386 for the measurement setup.
[18]S. Targonski and D. Pozar, in *Antennas and Propagation Society International Symposium, AP-S. Digest* (1996), Vol. 2, pp. 1326–1329.
[19]N. Yu, P. Genevet, M. Kats, F. Aieta, J. Tetienne, F. Capasso, and Z. Gaburro, Science **334**, 333 (2011).
[20]P. Nayeri, F. Yang, and A. Z. Elsherbeni, in *2011 IEEE International Symposium on Antennas and Propagation (APSURSI)* (IEEE, 2011), pp. 365–368.
[21]L. Josefsson and P. Persson, *Conformal Array Antenna Theory and Design* (John Wiley & Sons, 2006).
[22]M. Yi, W. Lee, and J. So, Electron. Lett. **50**, 1409 (2014).
[23]P. Padilla, A. Muñoz-Acevedo, M. Sierra-Castañer, and M. Sierra-Pérez, IEEE Trans. Antennas Propag. **58**, 2571 (2010).
[24]B. Memarzadeh and H. Mosallaei, Opt. Lett. **36**, 2569 (2011).
[25]J. Y. Lau and S. V. Hum, IEEE Trans. Antennas Propag. **60**, 5679 (2012).
[26]C. Pfeiffer and A. Grbic, IEEE Trans. Microwave Theory Tech. **61**, 4407 (2013).